C. R. Chimie 15 (2012) 962–968

Contents lists available at SciVerse ScienceDirect

Comptes Rendus Chimie

www.sciencedirect.com

Full paper/Mémoire

A novel catalyst for alkylation of benzene

Hossein Faghihian *, Mohammad Hadi Mohammadi

Department of Chemistry, University of Isfahan, Isfahan 81746-73441, Iran

ARTICLE INFO

Article history:
Received 16 May 2012
Accepted after revision 13 August 2012
Available online 19 September 2012

Keywords:
Al-pillared acid-activated clay
Solid-acid catalyst
Bentonite
Linear alkyl benzene
1-decene

ABSTRACT

In this research, acid-activated and pillared montmorillonite were prepared as catalysts for alkylation of benzene with 1-decene for production of linear alkyl bebzene (LAB). The catalysts were characterized by X-ray diffraction (XRD), FT-IR spectroscopy, scanning electron microscopy (SEM), N_2 adsorption-desorption isotherms, temperature programmed desorption (TPD) of NH_3 and elemental and thermal analysis techniques. The reaction conditions were optimized by varying catalyst concentration, reactants ratio and temperature in a batch-slurry reactor. It was found that acid-activation increased the porosity and surface acidity of the catalysts. Pillaring of the sample improved the surface area, micro-mesoporosity and acidity. Under optimized conditions more than 98% conversion of 1-decene was observed. All products were LABs and no major side reaction was observed.

1. Introduction

Alkylation of benzene with linear alkenes is used to synthesis linear alkyl benzenes (LABs) as primary material for production of detergent intermediate. Conventional process for LAB production is based on using highly corrosive and dangerous Lewis and Bronsted acid catalysts such as aluminum trichloride and hydrofluoric acid. Therefore, many efforts are being made to find efficient, recyclable and environmental friendly solid-acid catalysts [1,2]. Application of solid-acid catalysts removes the need for quench step, facilitating catalyst reuse and are generally much safer and easier to handle [3]. The efforts to find catalysts with high activity, low deactivation, and thermal stability have motivated the study of new materials. Acidic clays [4–6], heteropoly acids [7,8], zirconia supported 2-tungstophosphoric acid [9] and various microporous zeolites [10–14] have already been used for benzene alkylation. Among natural clays, montmorillonite due to its potential for interlayer modification and cation exchange is considered as an active material with interesting physicochemical properties. Montmorillonite is dioctahedral clay of smectite group and is composed of stacked aluminosilicate layers. When the mineral is acid-activated, hydrogen ions attack the aluminosilicate layers via the interlayer regions and the structure, chemical composition and physical properties of the clay will be seriously affected [15]. Acid-activation of clays is widely accepted as a feasible way to improve the acidity, particularly Bronsted acidity originated by the interaction of water molecules with Al^{3+} sites [16]. Acidity enhancement always followed by the increase of the pore volume and specific surface area [17,18].

Pillared clays can be synthesized by intercalating polycations into the interlayer region of expandable of the minerals. By calcinations, the polycations are converted to metal oxide pillar, which is fixed to the layers of the clay and yielding rigid cross-linked materials with permanent microprosity. Pillaring of clays increase the surface area and pore volume, and expose the acid sites of the interlayer region to reactant molecules.

In this work the catalytic activity of pillared acid-activated natural montmorillonite was studied in alkylation of benzene with α-olefin.

* Corresponding author.
E-mail address: Faghihian@iaush.ac.ir (H. Faghihian).

1631-0748/$ – see front matter © 2012 Académie des sciences. Published by Elsevier Masson SAS. All rights reserved.
http://dx.doi.org/10.1016/j.crci.2012.08.007

2. Experimental

2.1. Materials

H_2SO_4 (95–98%), NaOH, aluminum chloride ($AlCl_3$, $6H_2O$, 99%), 1-decene and benzene (99%) were purchased from Merck Company. All chemicals were research grade and used as received without further purification. Natural bentonite (sodium montmorillonite) was supplied by Amin Barq Company (Yazd, Iran).

2.2. Preparation

The sample was fractionated by sedimentation ($< 2\,\mu m$), purified by classical "gentle" purification method [19]. To prepare acid-activated sample (H-Clay), 30 g of purified bentonite was stirred with 175 mL of H_2SO_4 (4 M) for 2 h at 353 K in a round-bottom flask. The slurry was cooled, centrifuged and washed with distilled water until free of SO_4^{2-} ions, as tested by $BaCl_2$ solution.

Pillaring of the acid-activated sample was performed according to the method described by Chae et al. [20]. An adequate volume of 0.2 M NaOH was added dropwise to 0.2 M $AlCl_3$ solution under vigorous stirring to prepare aluminum hydroxy-oligomeric solution (OH/Al molar ratio of 2). After aging at room temperature for 24 h the appropriate amount of pillaring solution, required for the Al/clay (mmol Al/g clay) ratio of 25, was then slowly added to 1.0 L of distilled water containing 10 g of the acid-activated sample and stirred for 24 h. The solid was then centrifuged and washed repeatedly with de-ionized water until free of Cl^- ions (as tested by $AgNO_3$). The final product was dried at 383 K and calcined at 573 K for 3 h. The pillared sample was designated as H-Al-PILC.

2.3. Characterization techniques

The XRD patterns of the samples were obtained by a Bruker D8 ADVANCE, P4 PIONEER diffractometer, using CuKα radiation. FT-IR spectra were prepared using JASCO, FT-IR-6300 with a standard mid-IR DTGS detector. The specific surface area and total pore volume (TPV) of the samples were determined using N_2 as the sorbate at 77 K by a BELsorp max 113, Japan, Inc. system. Total specific surface areas were calculated using the Brunauer–Emmett–Teller (BET) equation. The TPV were evaluated from N_2 uptake at $P/P^\circ = 0.99$. The micropore size distribution of the samples was calculated using the Horvath–Kawazoe (H–K) equation [21] and the Barret, Johner and Halenda (BJH) method was used to determine the distributions of the mesopores [22]. The total acid site densities of the catalysts were measured by TPD of ammonia using a Micromeritics TPD/TPR 2900 instrument, equipped with a thermal conductivity detector (TCD). Chemical composition of the samples was determined by XRF method using a Bruker S4 PIONEER equipment. Thermal curves (Thermogravimetric (TG) and differential thermogravimetric (DTG)) were prepared using a Mettler, TG50 thermal analyzer under nitrogen atmosphere with a heating rate of 10 K min^{-1}. SEM was employed to examine the morphology of the samples by using a Philips XL SERIES, XL30 instrument. The cation exchange capacity (CEC) of the samples was determined by the method reported by Bergaya and Vayer [23].

2.4. Catalytic activity

H-Clay and H-Al-PILC catalysts were used for alkylation of benzene with 1-decene in a batch-slurry reactor at different temperatures of 388, 403 and 488 K. In each experiment, 1 wt% of the catalyst was used with a mixtures of benzene to olefin with different molar ratios of 8.75, 12 and 15. The alkylation products were analyzed by a FISONS GC 8000 series gas chromatograph with a DB-17 capillary column coupled to a flame ionization detector (FID).

3. Results and discussion

3.1. Characterization of the catalyst

In acid-activated sample considerable decrease in Al, Mg, and Fe content and an increase in SiO_2 was observed (Table 1). During acid treatment, the octahedral cations are washed out whereas thetrahedral silicon remained in the structure.

Replacement of interlayer cation by H^+ as a consequence of acid treatment reduced the CEC of the purified clay from 68.04 to 33.76 meq/100 g. Again in the pillared sample, the CEC value decreased to 15.31 meq/100 g, indicating that the exchangeable cations are mostly replaced by the pillars. The increase in Al content of H-Al-PILC sample confirmed this replacement (Table 1).

XRD patterns of the samples are given in Fig. 1. The purified sample contains montmorillonite with the basal spacing (d_{001}) of 1.22 nm as the dominant phase. In addition, calcite, talc, quartz and cristobalite were detected as impurities. In the acid-activated sample, the intensity of the 001 line ($2\theta = 6.8^\circ$) decreased and the characteristic lines of quartz and cristobalite are preserved, whereas the diffraction lines of calcite and talc disappeared. By

Table 1
Chemical compositions of the samples.

Compound	(W/W %)		
	Clay	H-Clay	H-Al-PILC
SiO_2	69.08	73.00	68.30
Al_2O_3	13.21	10.80	15.84
Fe_2O_3	2.21	1.56	1.39
MgO	1.78	0.86	0.79
Na_2O	0.40	0.16	0.23
CaO	1.17	0.98	0.21
K_2O	0.88	0.54	0.44
TiO_2	0.16	0.18	0.16
LOI[a]	11.31	11.67	12.48
CEC[b]	68.04	33.76	15.31

CEC: cation exchange capacity.
[a] Loss on ignition determined by DTG method.
[b] (meq/100g) determined by Cu ethylendiamin complex.

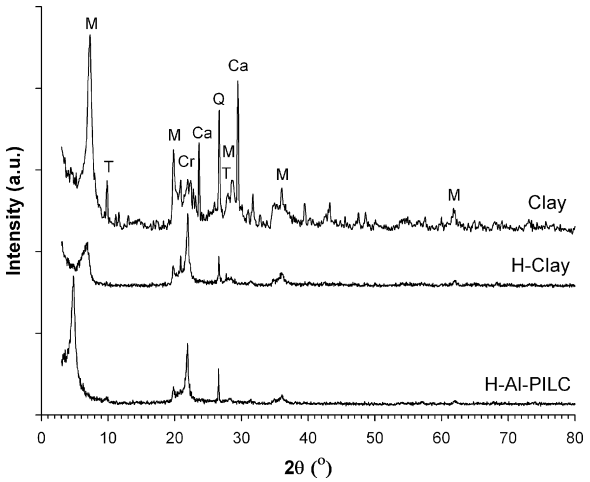

Fig. 1. X-ray diffraction paterns of the samples (M: montmorillonite, Q: qurtz, Ca: calcit, Cr: cristobalite, T: talc).

Table 2
Brunauer–Emmett–Teller specific surface area (S_{BET}), total pore volume (TPV), acidity and basal spacing (d_{001}) of the samples.

Sample	S_{BET} (m^2g^{-1})	TPV[a] (cm^3g^{-1})	Acidity (meq NH_3g^{-1})	$d_{(001)}$[b] (Å)
Clay	45.0	0.140	0.04	12.16
H-Clay	95.6	0.291	0.73	13.04
H-Al-PILC	158.3	0.298	1.05	18.38

[a] Total pore volume measured at $P/P^{\circ} = 0.99$.
[b] Obtained from XRD data.

comparison of purified and acid-activated samples, it was revealed that, although the crystallinity of the parent clay was decreased, its crystal structure was preserved. In pillared sample, the 001 line was shifted to smaller angle indicating the enlargement of the basal spacing ($d = 1.84$ nm) of the sample as a consequence of the pillaring process (Table 2).

The FT-IR spectrum of the purified clay (Fig. 2a) showed an intensive band at 1045 cm^{-1} which is attributed to the Si–O in-plan stretching vibration and moderate bands at 526 and 470 cm^{-1} assigned to Al–O–Si (octahedral Al) and Si–O–Si bending vibrations, respectively. The strong band around 1100 cm^{-1} together with a shoulder at 1190 cm^{-1} confirmed the presence of the silica phase, as observed in the XRD patterns. Stretching vibration of the hydroxyl groups of water molecules appeared at 3438 cm^{-1}. The band at 3623 cm^{-1} is assigned to hydroxyl groups coordinated to octahedral Al^{3+} [24].

Three peaks in the hydroxyl bending region at 920 cm^{-1} for Al_2OH, 875 cm^{-1} for AlFeOH, and 840 cm^{-1} for AlMgOH reflect that octahedral Al^{3+} is partially replaced by Fe^{3+} and Mg^{2+}. Furthermore, the band at 793 cm^{-1} reflect the presence of cristobalite and the shoulder near 620 cm^{-1} is attributed to the Al–O–R (R = Al and Mg) vibration of octahedral atoms [25].

In the FT-IR spectra of the acid-activated sample (Fig. 2b) the position and the shape of the bands are slightly changed. The band at 1045 cm^{-1} is shifted to higher wavenumbers ($\Delta\nu = 5$ cm^{-1}). The intensity of the hydroxyl bending vibration at 840 cm^{-1} (Al-Mg-OH) and 875 cm^{-1} (Al-Fe-OH) was significantly decreased. This was related to a decrease in Mg^{2+} and Fe^{2+} content and in agreement with chemical analysis results. In acid-activated sample, the intensity of the band at 793 cm^{-1} attributed to cristobalite was increased. This was also in agreement of chemical analysis data.

In the pillared sample (Fig. 2c), the band at 3438 cm^{-1} was broadened, indicating the introduction of the OH groups of the pillars and is interpreted as the effect of pillaring [26]. The increase in the broadness and intensity of the band at 3438 cm^{-1} is related to the presence of aluminum oxocations in the samples which increase the positive surface charge on oxygen involved in Si-O-Si linkages. The introduction of more positively charged aluminum groups causes a change in the electric field around Si groups and consequently a change in the symmetry of the surface Si-O-Si vibration could happen

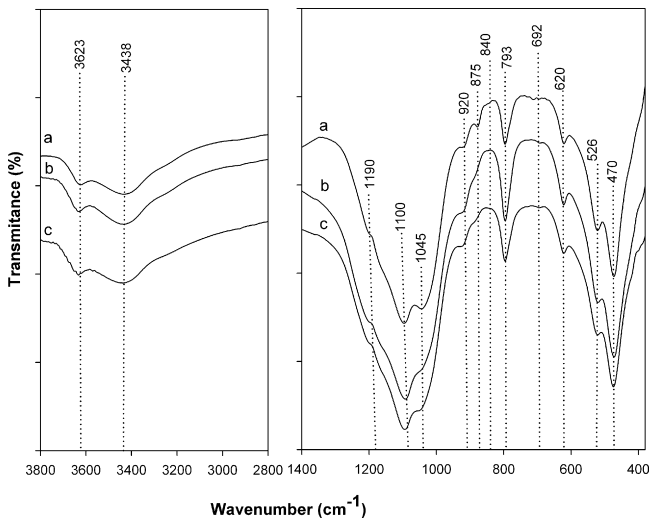

Fig. 2. FT-IR spectra of purified clay (a), H-Clay (b), H-Al-PILC (c).

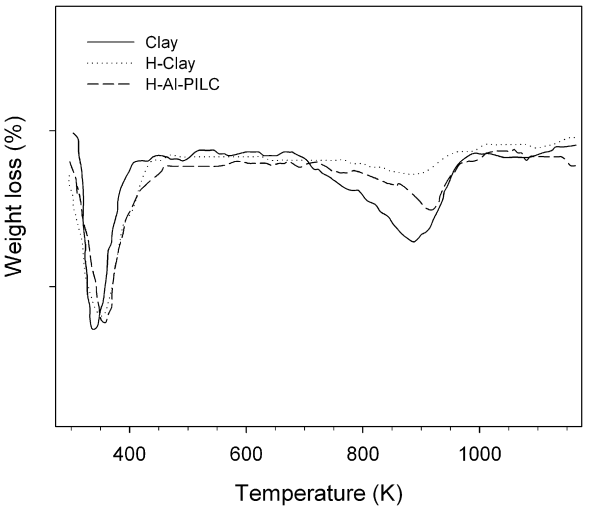

Fig. 3. DTG curves of purified clay, H-Clay and H-Al-PILC samples.

and the related stretching vibration band is shifted to a higher position [27].

Thermal behavior of purified clay, H-clay and H-Al-PILC samples was examined by DTG analysis (Fig. 3). Two distinct weight-loss regions around 373 and 923 K were observed in the thermal curves of all samples, which are respectively attributed to the dehydration (physically adsorbed water) and dehydroxylation (chemically bound OH groups). Between 373 and 923 K, a modest weight-loss was observed and this is attributed to the removal of interlayer water and onset of dehydroxylation [28]. The total weight-loss for the pillared sample was greater, which may be attributed to dehydration and dehydroxylation of both clay structure and the Al pillars. The total weight losses of samples are given in Table 1.

Fig. 4 shows the nitrogen adsorption-desorption isotherms of the samples. According to the International Union of Pure and Applied Chemistry (IUPAC) classification the isotherms are of IV type with a well defined H4 hysteresis loop denoting a slit-shaped porosity between plate-like particles. H4 hysteresis loops are generally observed with complex materials containing both micropores and mesopores [29]. By acid treatment, the cations are replaced by hydrogen ions and mesopores are increased, consequently the specific surface area and TPV of the sample sharply increased (Table 2). Compared to the parent bentonite, negligible change in micropore structure has occurred after acid treatment. By pillaring, the specific surface area was again increased by increasing separating contiguous layer distance (basal spacing of 1.84 nm). Mesopores are increased and partial transformation of mesopores to micropores during the intercalating process had occurred. Thus, H-Al-PILC possesses higher porosity and higher accessible specific surface area (Table 2). It was concluded that the acid-activated samples have no significant micropores whereas in pillared acid-activated samples, amount of micropores was increased. This would improve the accessibility of the active sites to the chemical reagents.

The acidity of the purified clay originates from two sources:

- compensating cations in the interlayer spaces that are mostly not easily accessible;
- specific sites at the layer edges; compensated by OH groups leading to Bronsted acid sites such as Si–OH and also coordinately unsaturated Al^{3+} and Mg^{2+} easily formed at the edges, behave as Lewis acid sites [30].

After acid-activation the protons replace the exchangeable cations and increase acidity [31]. By loading Lewis acid salts such as Al^{3+} the number of acid sites is also

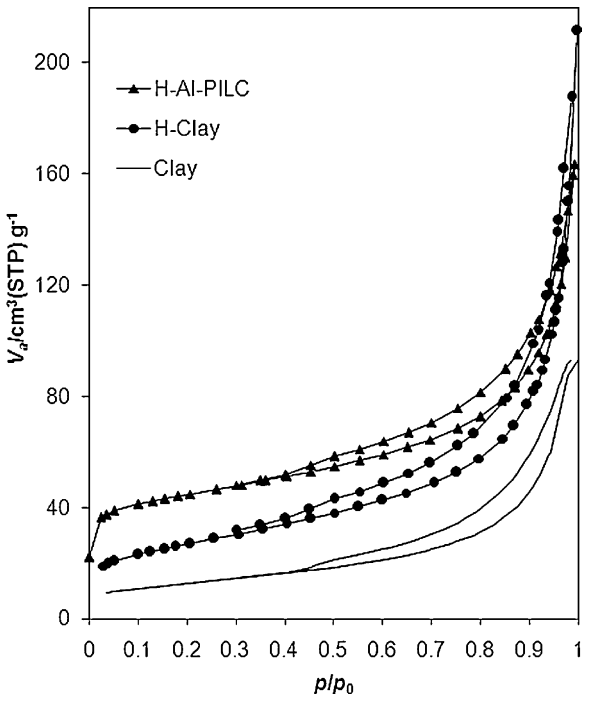

Fig. 4. Nitrogen adsorption-desorption isotherms of the samples.

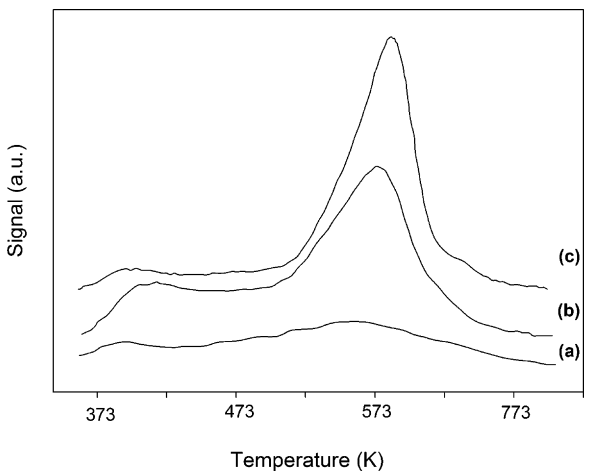

Fig. 5. NH3 TPD curves of the samples: purified clay (a), H-Clay (b), H-Al-PILC (c).

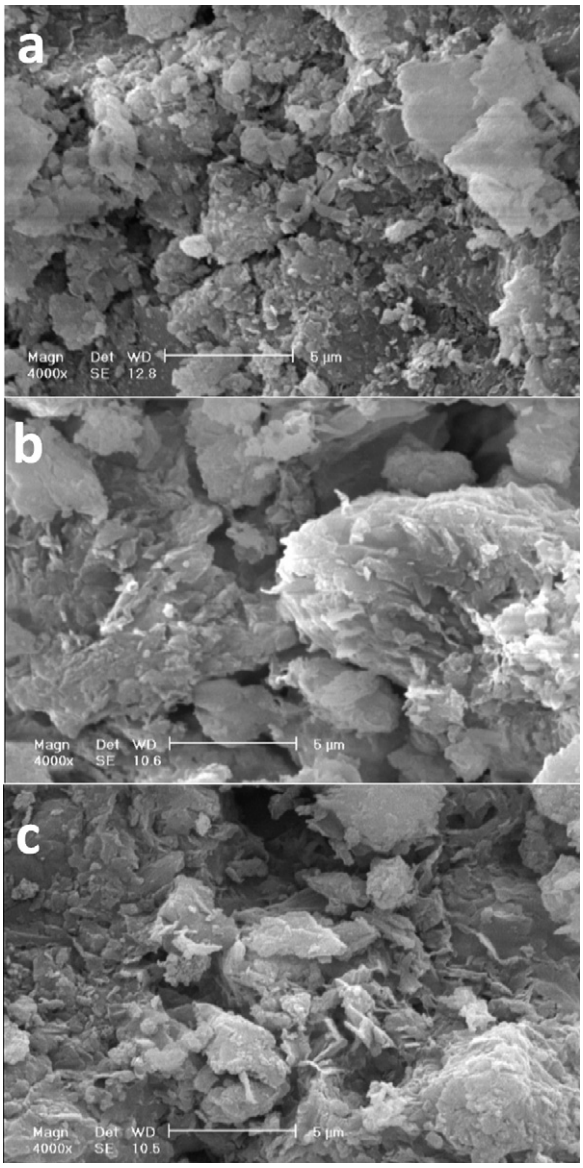

Fig. 6. Scanning electron microscopy images of the samples: purified clay (a), H-Clay (b), H-Al-PILC (c).

increased. Therefore, the total acidity of the H-Al-PILC sample was higher than that of the H-Clay sample. The result of TPD measurements (Fig. 5) showed that the number of acid sites of the samples is enhanced by acid treatment and pillaring processes (Table 2).

SEM images of the samples are shown in Fig. 6. In the SEM image of bentonite, thick aggregates with irregular shape and flake-shape were observed (Fig. 6a). After acid treatment the particles become smaller and thinner but the lamellar structure of bentonite still remained (Fig. 6b). In the H-Al-PILC sample (Fig. 6c), leaf-like agglomerates are observed. The morphological change of the sample indicated that Al_{13}^{7+} ions are incorporated into the interlayer space of acid-activated samples.

3.2. Activities of the catalysts

The catalytic activity of the samples was examined for alkylation of benzene with 1-decene. Alkylation of benzene with olefins is commonly considered as proceeding via a carbenium ion mechanism. Over the acid catalyst firstly, 1-decene forms a carbenium ion, and then undergoes a rapid double bond migration, and finally LABs (2-, 3-, 4- and 5-phenyldecane) are formed [32]. The alkylation reactions can be accompanied by side reactions, such as oligomerization of the olefin and alkylation with both monomer and the oligomers. For an industrial application high selectivity for linear 2- and 3-phenyl isomer is the major target, as this isomer yields detergents with desirable emulsifying and biodegradability properties [2].

3.2.1. Effect of molar ratio

Catalyst performance at different molar ratios is shown in Table 3a. 1-decene conversion of H-Al-PILC is higher than the H-Clay sample. This is in agreement with acidity enhancement of the sample and confirming the role of acidic sites in alkylation products.

In the pillared sample, nearly complete conversion was achieved with molar ratio of 15:1 and the conversion of 77.65% was observed with the benzene to olefin molar ratio of 8.75:1 (industrial scale ratio). The conversion percentage obtained by the H-Al-PILC sample is higher than the values reported by Thomas et al. [33] for H-Y and H-MOR zeolites, K-10 clay and SiO_2-Al_2O_3, and by Perego and Ingallina [34] for L zeolite and Al-PILC (Table 3b). Poly alkyl benzenes and tetralines are the typical compounds produced by benzene side reactions, while branched alkyl benzenes and oligomers are usually produced by olefin side reactions. Polyalkylation and oligomerization reactions are depressed by increasing the benzene to olefin ratio in the feed; as a general feature, the processes are designed, by controlling the reaction conditions, to minimize skeletal isomerization of the olefins, since high linearity is necessary to yield a biodegradable product. In the H-Al-PILC sample, complete conversion of 1-decene produced linear isomers of 2-, 3-, 4- and 5-phenyldecane and side reactions were not detected. Performance of H-Al-PILC catalyst for production of monoalkylate products was superior than the results obtained for H-Y, H-MOR, L and Beta zeolites, K-10 clay and SiO_2-Al_2O_3 reported by Thomas et al. [33], conventional Al-PILC reported by Perego and Ingallina (Table 3b) [34].

Formation of different monoalkylate isomers is caused by the intermediate carbenium ion isomerization. Effect of the different catalysts in the distribution of monoalkylated isomers is illustrated in Fig. 7. It is evident that 2-phenyldecane isomer has higher abundance between the monoalkylated isomers.

3.2.2. Effect of reaction temperature

The effect of temperature on the conversion and selectivity was studied at 388, 403 and 418 K (Table 4). The molar ratio of 15:1 (optimized value) was selected for the experiment. Although the catalysts showed enhanced activity at higher temperature, significant decrease of

Table 3
The effect of benzene to olefin molar ratio on alkylation reaction (T = 418 K; catalyst weight = 1 wt%, t = 4.5 h) of this work (a) and the results reported by the other workers (b).

(a) Sample	Benzene: olefin molar ratio					
	8.75:1[a]		12:1		15:1	
	1-decene conversion (%)	LAB[b] yield (%)	1-decene conversion (%)	LAB yield (%)	1-decene conversion (%)	LAB yield (%)
H-Clay	54.24	> 98.50	66.92	> 99.00	79.78	> 99.00
H-Al-PILC	77.65	> 98.50	95.17	> 99.00	> 98.00	> 99.00

(b) Sample	Conv. (%)	LAB yield (%)	Conditions	Reference
H-Y	79.5	90.4	T = 448 K, Benzen:1-decen; 20:1, t = 3 h	[33]
H-MOR	84.2	93.8	T = 448 K, Benzen:1-decen; 20:1, t = 3 h	[33]
K-10 Clay	38.9	93.1	T = 448 K, Benzen:1-decen; 20:1, t = 3 h	[33]
SiO_2-Al_2O_3	27.4	95.9	T = 448 K, Benzen:1-decen; 20:1, t = 3 h	[33]
L zeolite	92.8	72.9	T = 428 K, Benzen:1-decen; 15:1, t < 20 h	[34]
Al-PILC	93.1	98.5	T = 428 K, Benzen:1-decen; 15:1, t = 16 h	[34]

LAB: linear alkyl bebzene.
[a] Industrial scale ratio.
[b] Monoalkylated (include 2, 3, 4, and 5- phenyldecane isomers).

Table 4
Temperature effect on the activity and selectivity (catalyst weight = 1 wt%, benzene to olefin molar ratio = 15:1, t = 4.5 h).

Temperature	388 K		403 K		418 K	
Sample	Conv. (%)	2-φ Select. (%)	Conv. (%)	2-φ Select. (%)	Conv. (%)	2-φ Select. (%)
H-Clay	27.23	46.4	56.23	39.2	79.78	29.5
H-Al-PILC	26.72	44.9	59.54	39.3	> 98	33.3

2-phenyldecane selectivity was observed. The maximal selectivity was obtained at 388 K. A decrease of selectivity at higher temperature may be attributed to the fast equilibration of the olefin isomer (fast hydride shifts of the carbonium ion intermediate to produce the isomer ions) or rapid diffusion of the bulkiest LAB isomer out of the catalyst cavities [33], which increased the formation of other monoalkyalte isomers.

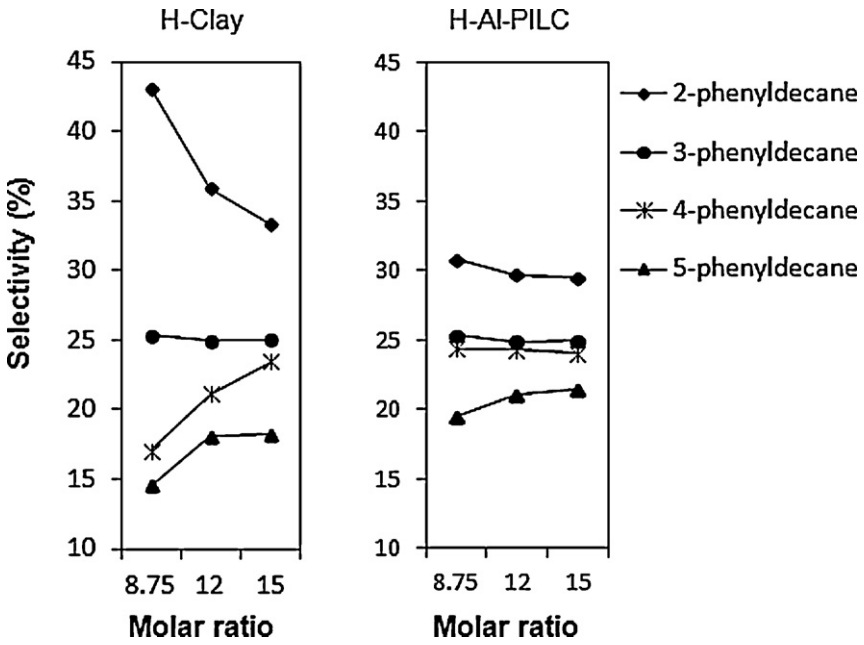

Fig. 7. Product selectivity of H-Clay and H-Al-PILC (catalyst weight = 1 wt%; T = 418 K; t = 4.5 h).

Table 5
The effect of catalyst weight on conversion and selectivity of H-Al-PILC (benzene to olefin molar ratio = 15:1, T = 418 K, t = 4.5 h).

Catalyst weight (wt%)	1-decene conversion (%)	2-φ selectivity (%)	LAB Yield (%)
0.25	74.91	32.8	99.1
0.50	86.23	32.4	99.3
1.00	> 98	33.3	99.4
1.25	> 98	32.4	99.3
1.75	> 98	33.6	99.2

LAB: linear alkyl bebzene.

3.3. Effect of catalyst amount

To examine the effect of the catalyst amount, a series of reactions were conducted by changing catalyst loading in the range of 0.25–1.75 wt % with molar ratio of 15 at 418 K for 4.5 h (Table 5). It was concluded that the conversion increased from 74.91 to more than 98% as the catalyst amount increased from 0.25 to 1 wt%. Beyond this amount, the conversion was steady because of deficiency of the reactant molecules.

4. Conclusion

Acid-activated and pillared bentonite was used for alkylation of benzene with 1-decene in a batch-slurry reactor. The specific surface area and the TPV of the catalyst was increased upon acid treatment. Intercalating of aluminum polyhydroxyl into the acid treated sample strongly increased the number of acid sites. Pillaring also improved specific surface area of the sample. The main advantage of the method is that no major side reactions, such as oligomerization of the olefin, dialkylation and higher alkyl benzene (HAB) happened, and the purity of the LAB products, which is an important parameter in LAB production industries, was enhanced. H-Al-PILC sample showed more than 98% conversion of 1-decene, which is beyond the values reported earlier for H-Y, H-MOR, L and Beta zeolites and conventional Al-PILC.

Acknowledgments

This study was completed at the University of Isfahan and supported by the Office of Graduate Studies. The authors are grateful to the office for their support.

Appendix A. Supplementary data

Supplementary data associated with this article can be found, in the online version, at http://dx.doi.org/10.1016/j.crci.2012.08.007.

References

[1] A. Corma, H. Garcia, Chem. Rev. 103 (2003) 4307.
[2] G.D. Yadav, M.I.N.I. Siddiqui, Ind. Eng. Chem. Res. 48 (2009) 10803.
[3] J.H. Clark, Green Chem. 1 (1999) 1.
[4] H. Ming Yuan, L. Zhonghui, M. Enze, Catal. Today 2 (1988) 321.
[5] A. De Stefanis, A.A.G. Tomlinson, Catal. Today 114 (2006) 126.
[6] S.R. Guerra, L. Merat, R.A.S. San Gil, L.C. Dieguez, Catal. Today 133 (2008) 223.
[7] T. Okuhara, N. Mizuno, M. Misono, Adv. Catal. 41 (1996) 113.
[8] C. Hu, Y. Zhang, L. Xu, G. Peng, Appl. Catal. A: Gen. 177 (1999) 237.
[9] B.M. Devassy, F. Lefebvre, S.B. Halligudi, J. Catal. 231 (2005) 1.
[10] J.L.G. de Almeida, M. Dufaux, Y.B. Taarit, C. Naccache, J. Am. Oil Chem. Soc. 71 (1994) 675.
[11] I. Craciun, M.F. Reyniers, G.B. Marin, J. Mol. Catal. A: Chem. 277 (2007) 1.
[12] Z. Da, Z. Han, P. Magnoux, M. Guisnet, Appl. Catal. A: Gen. 219 (2001) 45.
[13] M. Han, Z. Cui, C. Xu, W. Chen, Y. Jin, Appl. Catal. A: Gen. 238 (2003) 99.
[14] M. .Boveri, C. Marquez-Alvarez, M.A. Laborde, E. Sastre, Catal. Today 114 (2006) 217.
[15] R. Mokaya, W. Jones, M.E. Davies, M.E. Whittle, J. Solid State Chem. 111 (1994) 157.
[16] M. Bolognini, F.M. Cimini, L. Dal Pozzo, L. Maselli, D. Venerito, F. Pizzoli, G. Veronesi, C. R. Chimie 7 (2004) 143.
[17] R. Mokaya, W. Jones, M.E. Davies, M.E. Whittle, J. Am Oil Chem. Soc. 70 (1993) 241.
[18] P. Falaras, F. Lezou, G. Seiragakis, D. Petrakis, Clay Clay Miner 48 (2000) 549.
[19] K.A. Carrado, A., Decarreau, S., Petit, F., Bergaya, G. Lagaly, in: F. Bergaya, B.K.G., Theng, G. Lagaly (Eds.), Developments in Clay Science 1, Elsevier, Amsterdam, 2006, p. 115.
[20] H.J. Chae, I.S. Nam, S.W. Ham, S.B. Hong, Catal. Today 68 (2001) 31.
[21] G. Horvath, K.J. Kawazoe, Chem. Eng. Japan 16 (1983) 470.
[22] E.P. Barrett, L.G. Joyner, P.P. Halenda, J. Am. Chem. Soc. 73 (1951) 373.
[23] F. Bergaya, M. Vayer, Appl. Clay Sci. 12 (1997) 275.
[24] B. Tyagi, C.D. Chudasama, R.V. Jasra, Spectrochim. Acta A. 64 (2006) 273.
[25] A. Steudel, L.F. Batenburg, H.R. Fischer, P.G. Weidler, K. Emmerich, App. Clay Sci. 44 (2009) 105.
[26] M. Kurian, S. Sugunan, Indian J. Chem. A 42 (2003) 2480.
[27] P. Salerno, M.B. Asenjo, S. Mendioroz, Thermochim. Acta 379 (2001) 101.
[28] J.T. Kloprogge, E. Booij, J.B.H. Jansen, J.W. Geus, Clay Miner. 29 (1994) 153.
[29] K.S.W. Sing, D.H. Everett, L. Moscou, R.A. Pierrotti, J. Roquerol, T. Siemeniewska, Pure Appl. Chem. 57 (1985) 603.
[30] J.F. Lambert, G. Poncelet, Top. Catal. 4 (1997) 43.
[31] J.U. Kennedy Oubagaranadin, Z.V.P. Murthy, V.P. Mallapur, C. R. Chimie 13 (2010) 1359.
[32] J. Zhang, B. Chen, C. Li, Z. Zhu, L. Wen, E. Min, Appl. Catal. A: Gen. 249 (2003) 27.
[33] B. Thomas, B.B. Das, S. Sugunan, Micropor. Mesopor. Mat. 95 (2006) 329.
[34] C. Perego, P. Ingallina, Catal. Today 73 (2002) 3.